

Beamforming Design for IRS-and-UAV-aided Two-way Amplify-and-Forward Relay Networks

Xuehui Wang, Feng Shu, Yuanyuan Wu, Shihao Yan, Yifan Zhao, Qiankun Cheng,
and Jiangzhou Wang, *Fellow, IEEE*

Abstract—As a promising solution to improve communication quality, unmanned aerial vehicle (UAV) has been widely integrated into wireless networks. In this paper, for the sake of enhancing the message exchange rate between User1 (U_1) and User2 (U_2), an intelligent reflective surface (IRS)-and-UAV-assisted two-way amplify-and-forward (AF) relay wireless system is proposed, where U_1 and U_2 can communicate each other via a UAV-mounted IRS and an AF relay. Besides, an optimization problem of maximizing minimum rate is casted, where the variables, namely AF relay beamforming matrix and IRS phase shifts of two time slots, need to be optimized. To achieve a maximum rate, a low-complexity alternately iterative (AI) scheme based on zero forcing and successive convex approximation (LC-ZF-SCA) algorithm is put forward, where the expression of AF relay beamforming matrix can be derived in semi-closed form by ZF method, and IRS phase shift vectors of two time slots can be respectively optimized by utilizing SCA algorithm. To obtain a significant rate enhancement, a high-performance AI method based on one step, semidefinite programming and penalty SCA (ONS-SDP-PSCA) is proposed, where the beamforming matrix at AF relay can be firstly solved by singular value decomposition and ONS method, IRS phase shift matrices of two time slots are optimized by SDP and PSCA algorithms. Simulation results present that the rate performance of the proposed LC-ZF-SCA and ONS-SDP-PSCA methods surpass those of random phase and only AF relay. In particular, when total transmit power is equal to 30dBm, the proposed two methods can harvest more than 68.5% rate gain compared to random phase and only AF relay. Meanwhile, the rate performance of ONS-SDP-PSCA method at cost of extremely high complexity is superior to that of LC-ZF-SCA method.

Index Terms—Unmanned aerial vehicle, intelligent reflective surface, two-way amplify-and-forward relay, beamforming, phase shift, rate performance

I. INTRODUCTION

Because of a set of features of low cost, autonomy, mobility, high flexibility, and existence of line-of-sight (LoS) links,

This work was supported in part by the National Natural Science Foundation of China (Nos.U22A2002, and 62071234), the Hainan Province Science and Technology Special Fund (ZDKJ2021022), and the Scientific Research Fund Project of Hainan University under Grant KYQD(ZR)-21008. (*Corresponding authors: Yuanyuan Wu, Feng Shu*).

Xuehui Wang, Yuanyuan Wu, Yifan Zhao, and Qiankun Cheng are with the School of Information and Communication Engineering, Hainan University, Haikou, 570228, China.

Feng Shu is with the School of Information and Communication Engineering, Hainan University, Haikou 570228, China, and also with the School of Electronic and Optical Engineering, Nanjing University of Science and Technology, Nanjing 210094, China (e-mail: shufeng0101@163.com).

Shihao Yan is with the School of Science and Security Research Institute, Edith Cowan University, Perth, WA 6027, Australia (e-mail: s.yan@ecu.edu.au).

Jiangzhou Wang is with the School of Engineering, University of Kent, Canterbury CT2 7NT, U.K. (e-mail: j.z.wang@kent.ac.uk).

unmanned aerial vehicle (UAV) has been popularly applied to wireless network, so that high-rate and reliable transmission can be obtained [1]. With the ability to communicate and process signal, UAV can be regarded as a aerial base station (BS) or relay node to assist the key data collection and dissemination [2], [3]. So far, UAV has shown great potential in many civilian and commercial application scenarios, such as, search and rescue, aerial imaging, emergency care, traffic monitoring, three-dimensional (3D) reconstruction, and positioning [4], [5]. How to extend the coverage and improve the energy efficiency of multiple UAVs is always challenging. Based on spatial adaptive play, a energy-efficient coverage deployment algorithm was proposed in [6] to address two novel subproblems of maximum coverage and energy efficiency. Installing a light detection and ranging (LiDAR) sensor on the UAV can bring benefits for 3D reconstruction, while the mounting orientation of LiDAR is important. For a spinning LiDAR, its mounting orientation is generally suboptimal. In [7], its optimal installation angle along the vertical direction of UAV was derived. Since UAV is easy to be captured and attacked in particularly, it is difficult to ensure secure communication between UAV and BSs. To improve the security, the authors proposed a physically unclonable functions-based protocol in [8], where UAV and BSs need to be mutual authenticated. Although UAV can bring many conveniences to our lives because of unique characteristics, its size, power supply and weight are the constraints, which results in many challenges to UAV-enabled communication wireless networks, such as high-complexity power optimization and high-rate data transmission.

Very recently, due to the fact that intelligent reflecting surface (IRS) is able to intelligently regulate the propagation path of reflected signal without power consumption [9], IRS has been considered as a potential solution to meet the high-performance transmission requirement of wireless network [10]. IRS is a man-made plane, which consists of lots of passive and low-cost reflecting elements [11]. By flexibly deploying IRS on the surface of various buildings and tuning the reflection coefficient (i.e., amplitude and phase) of each unit [12], the uncontrollability of conventional wireless environment can be broken out, so that the signal coverage can be extended and the capacity of wireless network can be improved [13]. Because of a set of exclusive advantages, IRS has received increasing research mention from academia and industry. So far, IRS has been well studied in several UAV-aided communication scenarios [14]–[16]. IRS can be integrated to UAV network to promote air-ground communication.

The capacity of a flying IRS-aided UAV wireless network was derived in [14], where IRS elements were with certain phases before reflecting signal to UAV. The examination showed that phase error had a significant impact on the capacity. An IRS radio network based on UAV was presented in [16], where IRS was used to reflect signal transmitted by UAV to BS, so that UAV transmission can be improved. While meeting minimum master rate demand, a scheme based on relaxation was put forward to design IRS coefficient matrix, IRS scheduling, and UAV trajectory for minimum bit error rate.

In contrast to IRS, the traditional relay can also forward signal by using amplifying [17], decoding [18], compressing [19] and coding [20] strategies in uncontrollable communication environment, so that the received signal can be significantly enhanced to improve communication quality. Although the traditional relay has significant advantages in signal processing, it is an active forwarder which needs more costly hardware and circuit, higher energy and power consumption to improve rate performance compared to IRS [21], [22]. In [23], the researchers compared performance difference between the two wireless networks respectively assisted by IRS and decode-and-forward (DF) relay. It was demonstrated that the rate of the DF-aided system is higher than that of the IRS-aided network when the transmitter and receiver are far apart. However, the IRS-aided network is superior to the DF-aided system when the goal is to harvest maximum energy efficiency with minimum transmit power. At present, network coverage is still one of the most important and fundamental capabilities of communication systems. The deployment and operation costs of BSs in the fifth-generation (5G) mobile network have further increased compared to the fourth-generation (4G) network, and the electric charge of 5G BSs has brought a significant burden to operators. Consequently, it is urgent and imperative to research an innovative, efficient, high-rate, low-cost, and low-power-consumption solution for future wireless network.

Given that the advantages of IRS and relay, the combined network of IRS and relay is extremely attractive [24]–[30], which is considered as a win-win strategy in perspective of cost, spectrum and energy efficiency improvement, coverage extension and rate performance enhancement. In [25], multiple IRSs were applied to reflect signals in the DF relay network. In the case of perfect channel state information (CSI), the authors derived and analysed the network ergodic capacity by using the path loss model of Nakagami- m fading. Compare with a single IRS-aided DF relay system, the multi-IRS-assisted DF relay network could obtain rate gain by optimizing the numbers of IRSs and IRS units. A novel wireless network assisted by an IRS was proposed in [27], where the IRS controller was acted as a DF relay. By optimizing the time allocations of two time slots for the DF relay and passive beamforming at IRS, the coverage range and rate performance of the proposed novel network could be significantly improved. IRS deployment could affect the capacity of wireless network, there were two kinds of IRS-assisted DF relay networks were proposed in [29]. For the single-IRS-aided DF relay system, when the IRS was deployed near DF relay, it had a higher capacity compared to that case where deploying the IRS near

transceiver. For the multi-IRS-assisted DF relay network, three IRSs were respectively deployed near transmitter, DF relay, and receiver. By designing the cooperative beamforming of three IRSs, a larger capacity could be obtained.

To our best knowledge, with increasing attention paid to the hybrid network of relay and IRS, some corresponding work has emerged at present. While most of the research work on the combination network is focused on the DF relay, the research work on the hybrid network of amplify-and-forward (AF) relay and IRS is little. Additionally, IRS is fixed on tall buildings in most IRS-assisted wireless networks, which leads to limitations and inflexibility in the deployment of IRS. In particular, when the direct link from IRS to transceiver is obstructed, the rate performance and the coverage can be greatly affected, which results in poor communication for edge users. Or when an emergency occurs, if the communication quality cannot be guaranteed, the search and rescue activities can also be affected. To avoid the above mentioned cases, considering the unique characteristics of IRS, UAV, and AF relay, an IRS-and-UAV-aided two-way AF relay wireless network is proposed in this paper, where IRS is mounted to UAV. The contributions of this paper are summarized as follow:

- 1) A maximizing minimum rate optimization problem is established, where the transmit power of AF relay is limited and each IRS phase shift is need to meet the requirement of unit-modulus. Aiming to achieve a high information exchange rate, a low-complexity algorithm based on zero forcing and successive convex approximation (LC-ZF-SCA) is put forward to address the optimization problem by alternately optimizing one variable and fixing the other two variables. For AF relay beamforming matrix, its semi-closed expression can be derived by utilizing ZF method. For the optimization subproblem of IRS phase shift for the first or second time slots, SCA algorithm is applied to solve the non-convex subproblem given the other two variables. In contrast to random phase and only AF relay, the proposed LC-ZF-SCA method can achieve a 68.5% higher rate gain when total transmit power is 30dBm.
- 2) To achieve the goal of higher rate, a high-performance alternate algorithm based on one step, semidefinite programming and penalty SCA (ONS-SDP-PSCA) is proposed. Firstly, singular value decomposition (SVD) and ONS method are adopted to derive the semi-closed solution of AF relay beamforming matrix. Then, the optimization problem can be converted to a SDP problem. For the subproblem of IRS phase shift matrix in the second time slot, generalized fractional programming (GFP) is performed to convert constraints from non-convex to convex. Lastly, PSCA algorithm is used to tackle the subproblems of IRS phase shift matrices of two time slots. Compare with the proposed LC-ZF-SCA method, the proposed ONS-SDP-PSCA can obtain a significant rate enhancement especially in the high total transmit power region.

The rest of this article is arranged as follows. In Section II, we propose an IRS-and-UAV-assisted two-way AF relay

network, construct its system model and formulate optimization problem. In Section III, a low-complexity method is put forward to solve the optimization problem. In Section IV, a high-performance scheme is proposed to improve rate. The related numerical results are analyzed in Section V, and conclusions are shown in Section VI.

Notations: The letters of lower case, bold lower case, and bold upper case are used to denote scalars, vectors and matrices. The conjugate, transpose, conjugate transpose, Moore-Penrose pseudo inverse and trace of a matrix are respectively represented by $(\cdot)^*$, $(\cdot)^T$, $(\cdot)^H$, $(\cdot)^\dagger$ and $\text{tr}\{\cdot\}$. The expectation operation, absolute value, and 2-norm are respectively denoted as $\mathbb{E}\{\cdot\}$, $|\cdot|$, and $\|\cdot\|$. $\arg(\cdot)$ and $\Re(\cdot)$ stand for the phase and real part of a complex number, respectively. In addition, \mathbf{I}_M is a $M \times M$ identity matrix.

II. SYSTEM MODEL

A. Signal Model

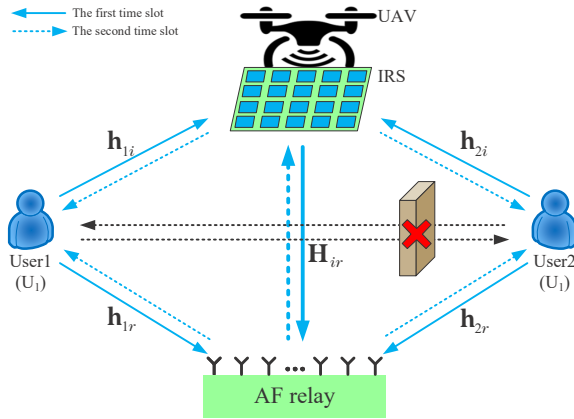


Fig. 1. An IRS-and-UAV-assisted two-way AF relay wireless network.

Fig. 1 sketches an IRS-and-UAV-aided two-way AF relay wireless network, where two single-antenna users can exchange their information via an AF relay and an IRS attached to UAV, the AF relay is equipped with M antennas while the IRS is made up of N passive reflecting elements. It is assumed that the UAV hovers and keeps static at a desired position, the direct link between two users is obstructed, and global CSI can be perfectly known.

In the first time slot, User1 (U_1) and User2 (U_2) simultaneously transmit their signal to AF relay. The received signal at AF relay can be denoted as

$$\mathbf{y}_r = \sqrt{P_1}(\mathbf{h}_{1r} + \mathbf{H}_{ir}\Theta_1\mathbf{h}_{1i})x_1 + \sqrt{P_2}(\mathbf{h}_{2r} + \mathbf{H}_{ir}\Theta_1\mathbf{h}_{2i})x_2 + \mathbf{n}_r, \quad (1)$$

where x_1 and x_2 are the independent signal from U_1 and U_2 , and $\mathbb{E}\{x_1^H x_1\} = \mathbb{E}\{x_2^H x_2\} = 1$. P_1 and P_2 respectively denote the transmit power of U_1 and U_2 . Without loss of generality, it is assumed that all channels follow Rayleigh fading. $\mathbf{h}_{1r} \in \mathbb{C}^{M \times 1}$, $\mathbf{h}_{1i} \in \mathbb{C}^{N \times 1}$, $\mathbf{h}_{2r} \in \mathbb{C}^{M \times 1}$, $\mathbf{h}_{2i} \in \mathbb{C}^{N \times 1}$ and $\mathbf{H}_{ir} \in \mathbb{C}^{M \times N}$ denote the frequency response of channel spanning from U_1 to AF relay, U_1 to IRS, U_2 to AF relay, U_2 to IRS and IRS to AF relay, respectively.

$\Theta_1 = \text{diag}(\alpha_{11}e^{j\theta_{11}}, \alpha_{12}e^{j\theta_{12}}, \dots, \alpha_{1N}e^{j\theta_{1N}})$ is the reflecting and configurable IRS matrix in the first time slot, where $\alpha_{1n} \in (0, 1]$ and $\theta_{1n} \in (0, 2\pi]$ respectively stand for the amplitude value and phase shift value of the n th reflection element. For simplicity, the amplitude value α_{1n} is generally set as 1. \mathbf{n}_r denotes the received additive white Gaussian noise (AWGN) at AF relay with $\mathbf{n}_r \sim \mathcal{CN}(0, \sigma_r^2 \mathbf{I}_M)$.

In the second time slot, performing receive and transmit beamforming operations on the received signal. Accordingly, the processed signal can be written as

$$\mathbf{x}_r = \mathbf{A}\mathbf{y}_r, \quad (2)$$

where $\mathbf{A} \in \mathbb{C}^{M \times M}$ is the beamforming matrix. AF relay transmit the processed signal to U_1 and U_2 , while the transmit power of AF relay is given by

$$P_r^t = P_1 \|\mathbf{A}(\mathbf{h}_{1r} + \mathbf{H}_{ir}\Theta_1\mathbf{h}_{1i})\|^2 + P_2 \|\mathbf{A}(\mathbf{h}_{2r} + \mathbf{H}_{ir}\Theta_1\mathbf{h}_{2i})\|^2 + \sigma_r^2 \|\mathbf{A}\|_F^2 \leq P_r, \quad (3)$$

where P_r represents the maximum transmit power of AF relay. The received signal at U_1 can be written as

$$\begin{aligned} y_{01} &= (\mathbf{h}_{1r}^H + \mathbf{h}_{1i}^H \Theta_2 \mathbf{H}_{ir}^H) \mathbf{A} \mathbf{y}_r + n_1 \\ &= \sqrt{P_1} (\mathbf{h}_{1r}^H + \mathbf{h}_{1i}^H \Theta_2 \mathbf{H}_{ir}^H) \mathbf{A} (\mathbf{h}_{1r} + \mathbf{H}_{ir} \Theta_1 \mathbf{h}_{1i}) x_1 \\ &\quad + \sqrt{P_2} (\mathbf{h}_{1r}^H + \mathbf{h}_{1i}^H \Theta_2 \mathbf{H}_{ir}^H) \mathbf{A} (\mathbf{h}_{2r} + \mathbf{H}_{ir} \Theta_1 \mathbf{h}_{2i}) x_2 \\ &\quad + (\mathbf{h}_{1r}^H + \mathbf{h}_{1i}^H \Theta_2 \mathbf{H}_{ir}^H) \mathbf{A} \mathbf{n}_r + n_1, \end{aligned} \quad (4)$$

where $\Theta_2 = \text{diag}(\alpha_{21}e^{j\theta_{21}}, \alpha_{22}e^{j\theta_{22}}, \dots, \alpha_{2N}e^{j\theta_{2N}})$ is the reflecting and configurable IRS matrix in the second time slot, where $\alpha_{2n} \in (0, 1]$ and $\theta_{2n} \in (0, 2\pi]$ are the amplitude value and phase shift value of the n th reflection element, respectively. Similarly, the amplitude value α_n is also equal to 1. n_1 is the received AWGN at U_1 with $n_1 \sim \mathcal{CN}(0, \sigma_1^2)$. Since U_1 has perfect knowledge of the signal transmitted by itself, the self-interference can be eliminated by subtracting the term about x_1 . After the self-interference elimination, the equivalent received signal at U_1 can be obtained as follows

$$y_1 = \sqrt{P_2} (\mathbf{h}_{1r}^H + \mathbf{h}_{1i}^H \Theta_2 \mathbf{H}_{ir}^H) \mathbf{A} (\mathbf{h}_{2r} + \mathbf{H}_{ir} \Theta_1 \mathbf{h}_{2i}) x_2 + (\mathbf{h}_{1r}^H + \mathbf{h}_{1i}^H \Theta_2 \mathbf{H}_{ir}^H) \mathbf{A} \mathbf{n}_r + n_1. \quad (5)$$

Similarly, the equivalent received signal at U_2 can be represented as follows

$$y_2 = \sqrt{P_1} (\mathbf{h}_{2r}^H + \mathbf{h}_{2i}^H \Theta_2 \mathbf{H}_{ir}^H) \mathbf{A} (\mathbf{h}_{1r} + \mathbf{H}_{ir} \Theta_1 \mathbf{h}_{1i}) x_1 + (\mathbf{h}_{2r}^H + \mathbf{h}_{2i}^H \Theta_2 \mathbf{H}_{ir}^H) \mathbf{A} \mathbf{n}_r + n_2, \quad (6)$$

where n_2 is the received AWGN at U_2 with $n_2 \sim \mathcal{CN}(0, \sigma_2^2)$.

The achievable rates at U_2 and U_1 can be respectively denoted as

$$R_{12} = \frac{1}{2} \log_2(1 + \text{SNR}_{12}), \quad (7)$$

$$R_{21} = \frac{1}{2} \log_2(1 + \text{SNR}_{21}), \quad (8)$$

where SNR_{12} and SNR_{21} are the received SNR at U_2 (i.e., from U_1 to U_2 link) and U_1 (i.e., from U_2 to U_1 link). SNR_{12} and SNR_{21} can be expressed as follow

$$\text{SNR}_{12} = \frac{P_1 |(\mathbf{h}_{2r}^H + \mathbf{h}_{2i}^H \Theta_2 \mathbf{H}_{ir}^H) \mathbf{A} (\mathbf{h}_{1r} + \mathbf{H}_{ir} \Theta_1 \mathbf{h}_{1i})|^2}{\|(\mathbf{h}_{2r}^H + \mathbf{h}_{2i}^H \Theta_2 \mathbf{H}_{ir}^H) \mathbf{A}\|^2 \sigma_r^2 + \sigma_2^2}, \quad (9)$$

$$\text{SNR}_{21} = \frac{P_2 |(\mathbf{h}_{1r}^H + \mathbf{h}_{1i}^H \Theta_1 \mathbf{H}_{ir}^H) \mathbf{A} (\mathbf{h}_{2r} + \mathbf{H}_{ir} \Theta_1 \mathbf{h}_{2i})|^2}{\|(\mathbf{h}_{1r}^H + \mathbf{h}_{1i}^H \Theta_1 \mathbf{H}_{ir}^H) \mathbf{A}\|^2 \sigma_r^2 + \sigma_1^2}. \quad (10)$$

The system rate is defined as

$$R = \min\{R_{12}, R_{21}\}. \quad (11)$$

B. Problem Formulation

The optimization problem of maximizing system rate is cast as

$$\max_{\mathbf{A}, \Theta_1, \Theta_2} \min\{R_{12}, R_{21}\} \quad (12a)$$

$$\text{s.t. } |\Theta_1(n, n)| = 1, |\Theta_2(n, n)| = 1, \forall n = 1, \dots, N, \quad (12b)$$

$$P_1 \|\mathbf{A} (\mathbf{h}_{1r} + \mathbf{H}_{ir} \Theta_1 \mathbf{h}_{1i})\|^2 + P_2 \|\mathbf{A} (\mathbf{h}_{2r} + \mathbf{H}_{ir} \Theta_1 \mathbf{h}_{2i})\|^2 + \sigma_r^2 \|\mathbf{A}\|_F^2 \leq P_r. \quad (12c)$$

Defining $\boldsymbol{\theta}_1 = [e^{j\theta_{11}}, e^{j\theta_{12}}, \dots, e^{j\theta_{1N}}]^T$, $\bar{\boldsymbol{\theta}}_1 = [\boldsymbol{\theta}_1; 1]$, $\boldsymbol{\theta}_2 = [e^{j\theta_{21}}, e^{j\theta_{22}}, \dots, e^{j\theta_{2N}}]^H$ and $\bar{\boldsymbol{\theta}}_2 = [\boldsymbol{\theta}_2; 1]$, we have $\mathbf{h}_{1r} + \mathbf{H}_{ir} \Theta_1 \mathbf{h}_{1i} = \mathbf{H}_1 \bar{\boldsymbol{\theta}}_1$, $\mathbf{h}_{2r} + \mathbf{H}_{ir} \Theta_1 \mathbf{h}_{2i} = \mathbf{H}_2 \bar{\boldsymbol{\theta}}_1$, $\mathbf{h}_{1r}^H + \mathbf{h}_{1i}^H \Theta_1 \mathbf{H}_{ir}^H = \bar{\boldsymbol{\theta}}_1^H \mathbf{H}_1^H$ and $\mathbf{h}_{2r}^H + \mathbf{h}_{2i}^H \Theta_1 \mathbf{H}_{ir}^H = \bar{\boldsymbol{\theta}}_1^H \mathbf{H}_2^H$, where $\mathbf{H}_1 = [\mathbf{H}_{ir} \text{diag}(\mathbf{h}_{1i}), \mathbf{h}_{1r}]$ and $\mathbf{H}_2 = [\mathbf{H}_{ir} \text{diag}(\mathbf{h}_{2i}), \mathbf{h}_{2r}]$. Accordingly, the optimization problem can be reformulated as

$$\max_{\mathbf{A}, \bar{\boldsymbol{\theta}}_1, \bar{\boldsymbol{\theta}}_2} \min\{R_{12}, R_{21}\} \quad (13a)$$

$$\text{s.t. } |\bar{\boldsymbol{\theta}}_1(n)| = 1, |\bar{\boldsymbol{\theta}}_2(n)| = 1, \forall n = 1, \dots, N, \quad (13b)$$

$$\bar{\boldsymbol{\theta}}_1(N+1) = 1, \bar{\boldsymbol{\theta}}_2(N+1) = 1, \quad (13c)$$

$$P_1 \|\mathbf{A} \mathbf{H}_1 \bar{\boldsymbol{\theta}}_1\|^2 + P_2 \|\mathbf{A} \mathbf{H}_2 \bar{\boldsymbol{\theta}}_1\|^2 + \sigma_r^2 \|\mathbf{A}\|_F^2 \leq P_r, \quad (13d)$$

where

$$R_{12} = \frac{1}{2} \log_2 \left(1 + \frac{P_1 |\bar{\boldsymbol{\theta}}_2^H \mathbf{H}_2^H \mathbf{A} \mathbf{H}_1 \bar{\boldsymbol{\theta}}_1|^2}{\|\bar{\boldsymbol{\theta}}_2^H \mathbf{H}_2^H \mathbf{A}\|^2 \sigma_r^2 + \sigma_2^2} \right), \quad (14)$$

$$R_{21} = \frac{1}{2} \log_2 \left(1 + \frac{P_2 |\bar{\boldsymbol{\theta}}_1^H \mathbf{H}_1^H \mathbf{A} \mathbf{H}_2 \bar{\boldsymbol{\theta}}_1|^2}{\|\bar{\boldsymbol{\theta}}_1^H \mathbf{H}_1^H \mathbf{A}\|^2 \sigma_r^2 + \sigma_1^2} \right). \quad (15)$$

Let us define a variable t , $R_{12} \geq t$ and $R_{21} \geq t$. According to the property of logarithmic function, problem (13) can be converted to

$$\max_{t, \mathbf{A}, \bar{\boldsymbol{\theta}}_1, \bar{\boldsymbol{\theta}}_2} t \quad (16a)$$

$$\text{s.t. } 2^{2t} \leq 1 + \frac{P_1 |\bar{\boldsymbol{\theta}}_2^H \mathbf{H}_2^H \mathbf{A} \mathbf{H}_1 \bar{\boldsymbol{\theta}}_1|^2}{\|\bar{\boldsymbol{\theta}}_2^H \mathbf{H}_2^H \mathbf{A}\|^2 \sigma_r^2 + \sigma_2^2}, \quad (16b)$$

$$2^{2t} \leq 1 + \frac{P_2 |\bar{\boldsymbol{\theta}}_1^H \mathbf{H}_1^H \mathbf{A} \mathbf{H}_2 \bar{\boldsymbol{\theta}}_1|^2}{\|\bar{\boldsymbol{\theta}}_1^H \mathbf{H}_1^H \mathbf{A}\|^2 \sigma_r^2 + \sigma_1^2}, \quad (16c)$$

$$(13b), (13c), (13d). \quad (16d)$$

It is too difficult to be solved directly because the variables, i.e., the beamforming matrix \mathbf{A} , the phase shift vector $\boldsymbol{\theta}_1$ and $\boldsymbol{\theta}_2$, are coupled with each other, which make the problem more

intractable. Here, there exist two alternating iteration schemes, namely LC-ZF-SCA and ONS-SDP-PSCA are proposed to tackle the optimization problem, and the related details are as follow.

III. PROPOSED LC-ZF-SCA-BASED METHOD

In the section, optimizing a variable or a group of variables given the remaining ones, there exist three subproblems need to be dealt with. In this case, a LC-ZF-SCA-based scheme is proposed to alternately optimize the variables \mathbf{A} , $\bar{\boldsymbol{\theta}}_1$ and $\bar{\boldsymbol{\theta}}_2$ for maximum rate. Here, ZF scheme is utilised to address the subproblem of calculating \mathbf{A} , where \mathbf{A} can be obtained in semi-closed form. For $\bar{\boldsymbol{\theta}}_1$ and $\bar{\boldsymbol{\theta}}_2$, we apply SCA algorithm to solve the corresponding two subproblems.

A. Optimization of \mathbf{A}

This subsection is aiming at obtaining beamforming matrix \mathbf{A} at AF relay with given $\bar{\boldsymbol{\theta}}_1$ and $\bar{\boldsymbol{\theta}}_2$. Since the computational complexity of directly optimizing the beamforming matrix is extremely high, we adopt a low complexity ZF scheme to obtain \mathbf{A} . Defining $\bar{\mathbf{H}}_1 \triangleq [\mathbf{H}_1 \bar{\boldsymbol{\theta}}_1, \mathbf{H}_2 \bar{\boldsymbol{\theta}}_1]$ and $\bar{\mathbf{H}}_2 \triangleq [\mathbf{H}_2 \bar{\boldsymbol{\theta}}_2, \mathbf{H}_1 \bar{\boldsymbol{\theta}}_2]^H$, in the light of ZF criterion [31], \mathbf{A} can be denoted as

$$\mathbf{A} = \tau \bar{\mathbf{H}}_2^\dagger \bar{\mathbf{H}}_1^\dagger. \quad (17)$$

Plugging (17) into the transmit power constraint with equality, we have

$$\tau = \sqrt{\frac{P_r}{P_1 \|\bar{\mathbf{H}}_2^\dagger \bar{\mathbf{H}}_1^\dagger \mathbf{H}_1 \bar{\boldsymbol{\theta}}_1\|^2 + P_2 \|\bar{\mathbf{H}}_2^\dagger \bar{\mathbf{H}}_1^\dagger \mathbf{H}_2 \bar{\boldsymbol{\theta}}_1\|^2 + \sigma_r^2 \|\bar{\mathbf{H}}_2^\dagger \bar{\mathbf{H}}_1^\dagger\|_F^2}}. \quad (18)$$

Thereby, the AF beamforming matrix \mathbf{A} can be obtained.

B. Optimization of $\bar{\boldsymbol{\theta}}_1$

Fixing $\bar{\boldsymbol{\theta}}_2$ and \mathbf{A} , problem (16) can be transformed to

$$\max_{t, \bar{\boldsymbol{\theta}}_1} t \quad (19a)$$

$$\text{s.t. } |\bar{\boldsymbol{\theta}}_1(n)| = 1, \forall n = 1, \dots, N, \bar{\boldsymbol{\theta}}_1(N+1) = 1, \quad (19b)$$

$$2^{2t} \leq 1 + \frac{\bar{\boldsymbol{\theta}}_1^H \mathbf{B}_{12} \bar{\boldsymbol{\theta}}_1}{\|\bar{\boldsymbol{\theta}}_2^H \mathbf{H}_2^H \mathbf{A}\|^2 \sigma_r^2 + \sigma_2^2}, \quad (19c)$$

$$2^{2t} \leq 1 + \frac{\bar{\boldsymbol{\theta}}_1^H \mathbf{B}_{21} \bar{\boldsymbol{\theta}}_1}{\|\bar{\boldsymbol{\theta}}_1^H \mathbf{H}_1^H \mathbf{A}\|^2 \sigma_r^2 + \sigma_1^2}, \quad (19d)$$

$$\bar{\boldsymbol{\theta}}_1^H (P_1 \mathbf{H}_1^H \mathbf{A}^H \mathbf{A} \mathbf{H}_1 + P_2 \mathbf{H}_2^H \mathbf{A}^H \mathbf{A} \mathbf{H}_2) \bar{\boldsymbol{\theta}}_1 + \sigma_r^2 \|\mathbf{A}\|_F^2 \leq P_r, \quad (19e)$$

where matrix $\mathbf{B}_{12} = P_1 \mathbf{H}_1^H \mathbf{A}^H \mathbf{H}_2 \bar{\boldsymbol{\theta}}_2 \bar{\boldsymbol{\theta}}_2^H \mathbf{H}_2^H \mathbf{A} \mathbf{H}_1$ and $\mathbf{B}_{21} = P_2 \mathbf{H}_2^H \mathbf{A}^H \mathbf{H}_1 \bar{\boldsymbol{\theta}}_1 \bar{\boldsymbol{\theta}}_1^H \mathbf{H}_1^H \mathbf{A} \mathbf{H}_2$. Constraint (19b), (19c) and (19d) are non-convex. Relaxing constraint (19b), we can obtain

$$\bar{\boldsymbol{\theta}}_1^H(n) \bar{\boldsymbol{\theta}}_1(n) \leq 1, \forall n = 1, \dots, N, \bar{\boldsymbol{\theta}}_1(N+1) = 1, \quad (20)$$

which is a convex constraint. In order to convert the constraint (19c) from non-convex to convex, the first-order Taylor approximation can be used to obtain the low bound of the

numerator of fraction in (19c). Its corresponding first-order Taylor expansion can be performed as follows

$$\bar{\boldsymbol{\theta}}_1^H \mathbf{B}_{12} \bar{\boldsymbol{\theta}}_1 \geq 2\Re\{\tilde{\boldsymbol{\theta}}_1^H \mathbf{B}_{12} \bar{\boldsymbol{\theta}}_1\} - \tilde{\boldsymbol{\theta}}_1^H \mathbf{B}_{12} \tilde{\boldsymbol{\theta}}_1, \quad (21)$$

where $\tilde{\boldsymbol{\theta}}_1$ is the feasible point. Similarly, performing first-order Taylor approximation operation on the numerator of fraction in (19d), we have

$$\bar{\boldsymbol{\theta}}_1^H \mathbf{B}_{21} \bar{\boldsymbol{\theta}}_1 \geq 2\Re\{\tilde{\boldsymbol{\theta}}_1^H \mathbf{B}_{21} \bar{\boldsymbol{\theta}}_1\} - \tilde{\boldsymbol{\theta}}_1^H \mathbf{B}_{21} \tilde{\boldsymbol{\theta}}_1. \quad (22)$$

Substituting (21) and (22) into constraint (19c) and (19d), the constraints can be respectively rewritten as

$$2^{2t} \leq 1 + \frac{2\Re\{\tilde{\boldsymbol{\theta}}_1^H \mathbf{B}_{12} \bar{\boldsymbol{\theta}}_1\} - \tilde{\boldsymbol{\theta}}_1^H \mathbf{B}_{12} \tilde{\boldsymbol{\theta}}_1}{\|\tilde{\boldsymbol{\theta}}_2^H \mathbf{H}_2^H \mathbf{A}\|^2 \sigma_r^2 + \sigma_2^2}, \quad (23)$$

$$2^{2t} \leq 1 + \frac{2\Re\{\tilde{\boldsymbol{\theta}}_1^H \mathbf{B}_{21} \bar{\boldsymbol{\theta}}_1\} - \tilde{\boldsymbol{\theta}}_1^H \mathbf{B}_{21} \tilde{\boldsymbol{\theta}}_1}{\|\tilde{\boldsymbol{\theta}}_2^H \mathbf{H}_1^H \mathbf{A}\|^2 \sigma_r^2 + \sigma_1^2}, \quad (24)$$

which are convex constraints. Therefore, the optimization problem (19) can be transformed to

$$\max_{t, \bar{\boldsymbol{\theta}}_1} t \quad (25a)$$

$$\text{s.t. (19e), (20), (23), (24).} \quad (25b)$$

Because of a linear objective function and several convex constraints, the above problem is convex, which can be solved by optimization solver, such as CVX. So the solution $\boldsymbol{\theta}_1$ is calculated as

$$\boldsymbol{\theta}_1 = e^{j \arg[\frac{\bar{\boldsymbol{\theta}}_1}{\bar{\boldsymbol{\theta}}_1^{(N+1)}} (1:N)]}. \quad (26)$$

C. Optimization of $\bar{\boldsymbol{\theta}}_2$

When $\bar{\boldsymbol{\theta}}_1$ and \mathbf{A} are given, the optimization problem (16) can be reduced to

$$\max_{t, \bar{\boldsymbol{\theta}}_2} t \quad (27a)$$

$$\text{s.t. } |\bar{\boldsymbol{\theta}}_2(n)| = 1, \forall n = 1, \dots, N, \bar{\boldsymbol{\theta}}_2(N+1) = 1, \quad (27b)$$

$$2^{2t} \leq 1 + \frac{P_1 |\bar{\boldsymbol{\theta}}_2^H \mathbf{H}_2^H \mathbf{A} \mathbf{H}_1 \bar{\boldsymbol{\theta}}_1|^2}{\|\bar{\boldsymbol{\theta}}_2^H \mathbf{H}_2^H \mathbf{A}\|^2 \sigma_r^2 + \sigma_2^2}, \quad (27c)$$

$$2^{2t} \leq 1 + \frac{P_2 |\bar{\boldsymbol{\theta}}_2^H \mathbf{H}_1^H \mathbf{A} \mathbf{H}_2 \bar{\boldsymbol{\theta}}_1|^2}{\|\bar{\boldsymbol{\theta}}_2^H \mathbf{H}_1^H \mathbf{A}\|^2 \sigma_r^2 + \sigma_1^2}, \quad (27d)$$

which is non-convex because of the non-convex constraint (27b), (27c) and (27d). For constraint (27b), a relaxation strategy similar to (20) can be performed as follows

$$\bar{\boldsymbol{\theta}}_2^H(n) \bar{\boldsymbol{\theta}}_2(n) \leq 1, \forall n = 1, \dots, N, \bar{\boldsymbol{\theta}}_2(N+1) = 1, \quad (28)$$

which is a convex constraint. For constraint (27c), its fraction part can be rewritten as follows

$$\frac{P_1 |\bar{\boldsymbol{\theta}}_2^H \mathbf{H}_2^H \mathbf{A} \mathbf{H}_1 \bar{\boldsymbol{\theta}}_1|^2}{\|\bar{\boldsymbol{\theta}}_2^H \mathbf{H}_2^H \mathbf{A}\|^2 \sigma_r^2 + \sigma_2^2} = \frac{\bar{\boldsymbol{\theta}}_2^H \mathbf{C}_{12} \bar{\boldsymbol{\theta}}_2}{\bar{\boldsymbol{\theta}}_2^H \mathbf{D}_{12} \bar{\boldsymbol{\theta}}_2}, \quad (29)$$

where matrix $\mathbf{C}_{12} = P_1 \mathbf{H}_2^H \mathbf{A} \mathbf{H}_1 \bar{\boldsymbol{\theta}}_1 \bar{\boldsymbol{\theta}}_1^H \mathbf{H}_1^H \mathbf{A}^H \mathbf{H}_2$ and $\mathbf{D}_{12} = \sigma_r^2 \mathbf{H}_2^H \mathbf{A} \mathbf{A}^H \mathbf{H}_2 + \begin{bmatrix} \mathbf{0}_{N \times N} & \mathbf{0}_{N \times 1} \\ \mathbf{0}_{1 \times N} & \sigma_2^2 \end{bmatrix}$. Substituting (29) into (27c) yields the following inequality

$$2^{2t} \leq 1 + \frac{\bar{\boldsymbol{\theta}}_2^H \mathbf{C}_{12} \bar{\boldsymbol{\theta}}_2}{\bar{\boldsymbol{\theta}}_2^H \mathbf{D}_{12} \bar{\boldsymbol{\theta}}_2}, \quad (30)$$

it is found that the above constraint is still non-convex. According to [32], the first-order Taylor expansion of (29) at a feasible point $\tilde{\boldsymbol{\theta}}_2$ can be expressed as follows

$$\frac{\bar{\boldsymbol{\theta}}_2^H \mathbf{C}_{12} \bar{\boldsymbol{\theta}}_2}{\bar{\boldsymbol{\theta}}_2^H \mathbf{D}_{12} \bar{\boldsymbol{\theta}}_2} \geq 2\Re\{\mathbf{f}_{12}^H \tilde{\boldsymbol{\theta}}_2\} + d_{12}, \quad (31)$$

where

$$\mathbf{f}_{12}^H = \frac{\tilde{\boldsymbol{\theta}}_2^H \mathbf{C}_{12}}{\tilde{\boldsymbol{\theta}}_2^H \mathbf{D}_{12} \tilde{\boldsymbol{\theta}}_2} - \tilde{\boldsymbol{\theta}}_2^H (\mathbf{D}_{12} - \lambda_{max}^{\mathbf{D}_{12}} \mathbf{I}_{N+1}) \frac{\tilde{\boldsymbol{\theta}}_2^H \mathbf{C}_{12} \tilde{\boldsymbol{\theta}}_2}{(\tilde{\boldsymbol{\theta}}_2^H \mathbf{D}_{12} \tilde{\boldsymbol{\theta}}_2)^2}, \quad (32)$$

$$d_{12} = -[2\lambda_{max}^{\mathbf{D}_{12}}(N+1) - \tilde{\boldsymbol{\theta}}_2^H \mathbf{D}_{12} \tilde{\boldsymbol{\theta}}_2] \frac{\tilde{\boldsymbol{\theta}}_2^H \mathbf{C}_{12} \tilde{\boldsymbol{\theta}}_2}{(\tilde{\boldsymbol{\theta}}_2^H \mathbf{D}_{12} \tilde{\boldsymbol{\theta}}_2)^2}, \quad (33)$$

and $\lambda_{max}^{\mathbf{D}_{12}}$ is the maximum eigenvalue of \mathbf{D}_{12} . Substituting the low bound of $\frac{\bar{\boldsymbol{\theta}}_2^H \mathbf{C}_{12} \bar{\boldsymbol{\theta}}_2}{\bar{\boldsymbol{\theta}}_2^H \mathbf{D}_{12} \bar{\boldsymbol{\theta}}_2}$, (32) and (33) into (30) yields

$$2^{2t} \leq 1 + 2\Re\{\mathbf{f}_{12}^H \tilde{\boldsymbol{\theta}}_2\} + d_{12}, \quad (34)$$

which is convex. In the same manner, for the fraction part of constraint (27d) we have

$$\frac{P_2 |\bar{\boldsymbol{\theta}}_2^H \mathbf{H}_1^H \mathbf{A} \mathbf{H}_2 \bar{\boldsymbol{\theta}}_1|^2}{\|\bar{\boldsymbol{\theta}}_2^H \mathbf{H}_1^H \mathbf{A}\|^2 \sigma_r^2 + \sigma_1^2} = \frac{\bar{\boldsymbol{\theta}}_2^H \mathbf{C}_{21} \bar{\boldsymbol{\theta}}_2}{\bar{\boldsymbol{\theta}}_2^H \mathbf{D}_{21} \bar{\boldsymbol{\theta}}_2} \geq 2\Re\{\mathbf{f}_{21}^H \tilde{\boldsymbol{\theta}}_2\} + d_{21}, \quad (35)$$

where matrix $\mathbf{C}_{21} = P_2 \mathbf{H}_1^H \mathbf{A} \mathbf{H}_2 \bar{\boldsymbol{\theta}}_1 \bar{\boldsymbol{\theta}}_1^H \mathbf{H}_2^H \mathbf{A}^H \mathbf{H}_1$, $\mathbf{D}_{21} = \sigma_r^2 \mathbf{H}_1^H \mathbf{A} \mathbf{A}^H \mathbf{H}_1 + \begin{bmatrix} \mathbf{0}_{N \times N} & \mathbf{0}_{N \times 1} \\ \mathbf{0}_{1 \times N} & \sigma_1^2 \end{bmatrix}$ and

$$\mathbf{f}_{21}^H = \frac{\tilde{\boldsymbol{\theta}}_2^H \mathbf{C}_{21}}{\tilde{\boldsymbol{\theta}}_2^H \mathbf{D}_{21} \tilde{\boldsymbol{\theta}}_2} - \tilde{\boldsymbol{\theta}}_2^H (\mathbf{D}_{21} - \lambda_{max}^{\mathbf{D}_{21}} \mathbf{I}_{N+1}) \frac{\tilde{\boldsymbol{\theta}}_2^H \mathbf{C}_{21} \tilde{\boldsymbol{\theta}}_2}{(\tilde{\boldsymbol{\theta}}_2^H \mathbf{D}_{21} \tilde{\boldsymbol{\theta}}_2)^2}, \quad (36)$$

$$d_{21} = -[2\lambda_{max}^{\mathbf{D}_{21}}(N+1) - \tilde{\boldsymbol{\theta}}_2^H \mathbf{D}_{21} \tilde{\boldsymbol{\theta}}_2] \frac{\tilde{\boldsymbol{\theta}}_2^H \mathbf{C}_{21} \tilde{\boldsymbol{\theta}}_2}{(\tilde{\boldsymbol{\theta}}_2^H \mathbf{D}_{21} \tilde{\boldsymbol{\theta}}_2)^2}. \quad (37)$$

Correspondingly, constraint (27d) can be transformed to be convex as follows

$$2^{2t} \leq 1 + 2\Re\{\mathbf{f}_{21}^H \tilde{\boldsymbol{\theta}}_2\} + d_{21}. \quad (38)$$

Therefore, the optimization problem (27) can be reformulated as follows

$$\max_{t, \bar{\boldsymbol{\theta}}_2} t \quad (39a)$$

$$\text{s.t. (28), (34), (38).} \quad (39b)$$

The solution $\bar{\boldsymbol{\theta}}_2$ can be directly solved by CVX optimization tool. Thereby, the solution $\boldsymbol{\theta}_2$ can be achieved as

$$\boldsymbol{\theta}_2 = e^{j \arg[\frac{\bar{\boldsymbol{\theta}}_2}{\bar{\boldsymbol{\theta}}_2^{(N+1)}} (1:N)]}. \quad (40)$$

D. Overall algorithm

The optimization problem have a upper bound because of the non-decreasing property and limited transmit power of U_1 , U_2 and AF relay. Performing alternative iteration among \mathbf{A} , $\boldsymbol{\theta}_1$ and $\boldsymbol{\theta}_2$ until the convergence criterion is satisfied. The proposed LC-ZF-SCA algorithm is summarized in the following Algorithm 1.

The computational complexity of LC-ZF-SCA algorithm contains three parts related to \mathbf{A} , $\bar{\boldsymbol{\theta}}_1$ and $\bar{\boldsymbol{\theta}}_2$. The complexity

Algorithm 1 Proposed LC-ZF-SCA algorithm

- 1: Initialize \mathbf{A}^0 , $\bar{\boldsymbol{\theta}}_1^0$ and $\bar{\boldsymbol{\theta}}_2^0$, R^0 can be calculated.
 - 2: Set the convergence error δ and initialize iteration number $i = 0$.
 - 3: **repeat**
 - 4: Given $(\bar{\boldsymbol{\theta}}_1^i, \bar{\boldsymbol{\theta}}_2^i)$, calculate \mathbf{A}^{i+1} with (17) and (18).
 - 5: Given $(\mathbf{A}^{i+1}, \bar{\boldsymbol{\theta}}_2^i)$, solve problem (25) to obtain $\bar{\boldsymbol{\theta}}_1^{i+1}$.
 - 6: Given $(\mathbf{A}^{i+1}, \bar{\boldsymbol{\theta}}_1^{i+1})$, solve problem (39) to obtain $\bar{\boldsymbol{\theta}}_2^{i+1}$.
 - 7: Calculate R^{i+1} by using $(\mathbf{A}^{i+1}, \bar{\boldsymbol{\theta}}_1^{i+1}, \bar{\boldsymbol{\theta}}_2^{i+1})$.
 - 8: $i = i + 1$.
 - 9: **until**
 - 10: $|R^{i+1} - R^i| \leq \delta$.
-

of \mathbf{A} is denoted as $M^3 + 11M^2 + 10MN + 7M + 6$ float-point operations (FLOPs) in line with (17) and (18). Since problem (39) has three linear constraints, one second-order cone (SOC) constraint of dimension $N + 1$ and one SOC constraint of dimension N , the complexity of calculating $\bar{\boldsymbol{\theta}}_1$ is denoted as $n_{\bar{\boldsymbol{\theta}}_1} \sqrt{7}[(N + 1)^2 + N^2 + n_{\bar{\boldsymbol{\theta}}_1}^2 + 3n_{\bar{\boldsymbol{\theta}}_1} + 3]$, where $n_{\bar{\boldsymbol{\theta}}_1} = N + 2$ is the number of variables. Besides, there are three linear constraints, one SOC constraint of dimension N and $N + 2$ variables in problem (39), its complexity is presented as $n_{\bar{\boldsymbol{\theta}}_2} \sqrt{5}[N^2 + n_{\bar{\boldsymbol{\theta}}_2}^2 + 3n_{\bar{\boldsymbol{\theta}}_2} + 3]$, where $n_{\bar{\boldsymbol{\theta}}_2} = N + 2$. Therefore, the complexity of LC-ZF-SCA algorithm is written as follows

$$\begin{aligned} & \mathcal{O}\{D_1[M^3 + 11M^2 + 10MN + 7M + 6 \\ & + n_{\bar{\boldsymbol{\theta}}_1} \sqrt{7}((N + 1)^2 + N^2 + n_{\bar{\boldsymbol{\theta}}_1}^2 + 3n_{\bar{\boldsymbol{\theta}}_1} + 3) \\ & + n_{\bar{\boldsymbol{\theta}}_2} \sqrt{5}(N^2 + n_{\bar{\boldsymbol{\theta}}_2}^2 + 3n_{\bar{\boldsymbol{\theta}}_2} + 3)] \ln(1/\varepsilon)\} \end{aligned} \quad (41)$$

FLOPs, where D_1 is the iterative number in Algorithm 1 and ε is the computation accuracy.

IV. PROPOSED ONS-SDP-PSCA-BASED METHOD

In the section III, the LC-ZF-SCA-based scheme is put forward to optimize AF relay beamforming matrix \mathbf{A} , IRS reflecting coefficient vectors $\boldsymbol{\theta}_1$ and $\boldsymbol{\theta}_2$. To obtain a rate performance improvement, a high-performance ONS-SDP-PSCA-based scheme is proposed, where the subproblem related to \mathbf{A} is solved by SVD and ONS method. Then the optimization problem is translated to two SDP problems, where IRS phase shift matrix in the second time slot is optimized by GFP algorithm, and a penalty function is adopted to recover rank-one IRS phase shift matrices of two time slots. The associated details are as follow.

A. Optimization of \mathbf{A}

Given $\bar{\boldsymbol{\theta}}_1$ and $\bar{\boldsymbol{\theta}}_2$, the SVD of $\bar{\mathbf{H}}_1$ and $\bar{\mathbf{H}}_2$ can be respectively expressed as follow

$$\begin{aligned} \bar{\mathbf{H}}_1 &= \mathbf{U}_1 \boldsymbol{\Sigma}_1 \mathbf{V}_1^H \\ &= [\mathbf{U}_{11} \ \mathbf{U}_{12}] \begin{bmatrix} \boldsymbol{\Sigma}_{11} \\ \boldsymbol{\Sigma}_{12} \end{bmatrix} \mathbf{V}_1^H \\ &= \mathbf{U}_{11} \boldsymbol{\Sigma}_{11} \mathbf{V}_1^H, \\ \bar{\mathbf{H}}_2 &= \mathbf{U}_2 \boldsymbol{\Sigma}_2 \mathbf{V}_2^H \\ &= \mathbf{U}_2 [\boldsymbol{\Sigma}_{21} \ \boldsymbol{\Sigma}_{22}] \begin{bmatrix} \mathbf{V}_{21}^H \\ \mathbf{V}_{22}^H \end{bmatrix} \\ &= \mathbf{U}_2 \boldsymbol{\Sigma}_{21} \mathbf{V}_{21}^H, \end{aligned} \quad (42)$$

where $\mathbf{U}_1 \in \mathbb{C}^{M \times M}$, $\mathbf{V}_1 \in \mathbb{C}^{2 \times 2}$, $\mathbf{U}_2 \in \mathbb{C}^{2 \times 2}$, and $\mathbf{V}_2 \in \mathbb{C}^{M \times M}$ are the unitary matrices, $\boldsymbol{\Sigma}_1 \in \mathbb{C}^{M \times 2}$ and $\boldsymbol{\Sigma}_2 \in \mathbb{C}^{2 \times M}$ are the matrices with singular values for elements on the main diagonal and 0 for other elements. $\mathbf{U}_{11} \in \mathbb{C}^{M \times 2}$, $\mathbf{U}_{12} \in \mathbb{C}^{M \times (M-2)}$, $\mathbf{V}_{21} \in \mathbb{C}^{M \times 2}$ and $\mathbf{V}_{22} \in \mathbb{C}^{M \times (M-2)}$, $\boldsymbol{\Sigma}_{11} \in \mathbb{C}^{2 \times 2}$ and $\boldsymbol{\Sigma}_{21} \in \mathbb{C}^{2 \times 2}$ are diagonal matrices consisting of singular values and $\boldsymbol{\Sigma}_{12} \in \mathbb{C}^{(M-2) \times 2}$ and $\boldsymbol{\Sigma}_{22} \in \mathbb{C}^{2 \times (M-2)}$ are zero matrices. The beamforming matrix \mathbf{A} can be structured as

$$\begin{aligned} \mathbf{A} &= \mathbf{V}_{21} \boldsymbol{\Omega} \mathbf{U}_{11}^H \\ &= \mathbf{V}_{21} \boldsymbol{\Lambda}_2 \mathbf{U}_2^H \mathbf{V}_1 \boldsymbol{\Lambda}_1 \mathbf{U}_{11}^H, \end{aligned} \quad (44)$$

where matrix $\boldsymbol{\Omega} \in \mathbb{C}^{2 \times 2}$, $\boldsymbol{\Lambda}_1 \in \mathbb{C}^{2 \times 2} \succeq \mathbf{0}$ and $\boldsymbol{\Lambda}_2 \in \mathbb{C}^{2 \times 2} \succeq \mathbf{0}$ are diagonal matrices. $\mathbf{V}_1 \boldsymbol{\Lambda}_1 \mathbf{U}_{11}^H$ denotes receive beamforming, $\mathbf{V}_{21} \boldsymbol{\Lambda}_2 \mathbf{U}_2^H$ represents transmit beamforming. While $\boldsymbol{\Lambda}_1$ and $\boldsymbol{\Lambda}_2$ are unknown, which are determined by searching more than four variables satisfying $\boldsymbol{\Lambda}_1 \succeq \mathbf{0}$ and $\boldsymbol{\Lambda}_2 \succeq \mathbf{0}$. Here, the one-step (ONS) method is used to solve $\boldsymbol{\Lambda}_1$ and $\boldsymbol{\Lambda}_2$ by selecting $\boldsymbol{\Lambda}_1 = \boldsymbol{\Lambda}_2 = \sqrt{\rho} \mathbf{I}_2$ [33], while the beamforming matrix \mathbf{A} can be obtained as

$$\mathbf{A} = \rho \mathbf{V}_{21} \mathbf{U}_2^H \mathbf{V}_1 \mathbf{U}_{11}^H = \rho \boldsymbol{\Upsilon}, \quad (45)$$

where ρ is need to meet transmit power constraint (47f) with equality. Particularly, ρ is chosen as follows

$$\begin{aligned} \rho &= \\ & \sqrt{\frac{P_r}{\text{tr}\{\bar{\boldsymbol{\Theta}}_1(P_1 \mathbf{H}_1^H \boldsymbol{\Upsilon}^H \boldsymbol{\Upsilon} \mathbf{H}_1 + P_2 \mathbf{H}_2^H \boldsymbol{\Upsilon}^H \boldsymbol{\Upsilon} \mathbf{H}_2)\} + \sigma_r^2 \|\boldsymbol{\Upsilon}\|_F^2}}}. \end{aligned} \quad (46)$$

B. Problem Reformulation

After that, problem (16) can be further translated to the following SDP problem

$$\max_{t, \mathbf{A}, \bar{\boldsymbol{\Theta}}_1, \bar{\boldsymbol{\Theta}}_2} t \quad (47a)$$

$$\text{s.t. } \bar{\boldsymbol{\Theta}}_1(n, n) = 1, \bar{\boldsymbol{\Theta}}_2(n, n) = 1, \forall n = 1, \dots, N + 1, \quad (47b)$$

$$\bar{\boldsymbol{\Theta}}_1 \succeq \mathbf{0}, \bar{\boldsymbol{\Theta}}_2 \succeq \mathbf{0}, \text{rank}(\bar{\boldsymbol{\Theta}}_1) = 1, \text{rank}(\bar{\boldsymbol{\Theta}}_2) = 1, \quad (47c)$$

$$2^{2t} \leq 1 + \frac{P_1 \text{tr}(\bar{\boldsymbol{\Theta}}_1 \mathbf{H}_1^H \mathbf{A}^H \mathbf{H}_2 \bar{\boldsymbol{\Theta}}_2 \mathbf{H}_2^H \mathbf{A} \mathbf{H}_1)}{\text{tr}(\bar{\boldsymbol{\Theta}}_2 \mathbf{D}_{12})}, \quad (47d)$$

$$2^{2t} \leq 1 + \frac{P_2 \text{tr}(\bar{\boldsymbol{\Theta}}_1 \mathbf{H}_2^H \mathbf{A}^H \mathbf{H}_1 \bar{\boldsymbol{\Theta}}_2 \mathbf{H}_1^H \mathbf{A} \mathbf{H}_2)}{\text{tr}(\bar{\boldsymbol{\Theta}}_2 \mathbf{D}_{21})}, \quad (47e)$$

$$\begin{aligned} & \text{tr}\{\bar{\boldsymbol{\Theta}}_1(P_1 \mathbf{H}_1^H \mathbf{A}^H \mathbf{A} \mathbf{H}_1 + P_2 \mathbf{H}_2^H \mathbf{A}^H \mathbf{A} \mathbf{H}_2)\} \\ & + \sigma_r^2 \|\mathbf{A}\|_F^2 \leq P_r, \end{aligned} \quad (47f)$$

where $\bar{\Theta}_1 = \bar{\theta}_1 \bar{\theta}_1^H$ and $\bar{\Theta}_2 = \bar{\theta}_2 \bar{\theta}_2^H$. Since \mathbf{A} , $\bar{\Theta}_1$, $\bar{\Theta}_2$ are coupled each other and there are two rank-one constraints, which results in a non-convex problem, and directly solving such a non-convex problem is difficult. Meanwhile, given that the semi-closed-form expression of \mathbf{A} in section IV-A has been obtained, the above mentioned problem (47) can be decomposed into two subproblems associated to $\bar{\Theta}_1$ and $\bar{\Theta}_2$. The following are the optimization details for obtaining rank-one $\bar{\Theta}_1$ and $\bar{\Theta}_2$.

C. Optimization of $\bar{\Theta}_1$

Fixing \mathbf{A} and $\bar{\Theta}_2$, the optimization problem (47) can be further translated to

$$\max_{t, \bar{\Theta}_1} t \quad (48a)$$

$$\text{s.t. } \bar{\Theta}_1(n, n) = 1, \forall n = 1, \dots, N+1, \quad (48b)$$

$$\bar{\Theta}_1 \succeq \mathbf{0}, \text{rank}(\bar{\Theta}_1) = 1, \quad (48c)$$

$$(47d), (47e), (47f). \quad (48d)$$

The constraint $\text{rank}(\bar{\Theta}_1) = 1$ leads the above problem to be non-convex. To convert the above problem to be convex, performing the following equivalent operation on $\text{rank}(\bar{\Theta}_1) = 1$

$$\text{tr}(\bar{\Theta}_1) - \lambda_{max}(\bar{\Theta}_1) \leq 0, \quad (49)$$

where $\lambda_{max}(\bar{\Theta}_1)$ is the maximum eigenvalue of $\bar{\Theta}_1$. Due to the constraint $\bar{\Theta}_1 \succeq \mathbf{0}$, it is implied that $\text{tr}(\bar{\Theta}_1) - \lambda_{max}(\bar{\Theta}_1) \geq 0$. In order to better address the problem of rank-one constraint, we adopt a penalty method to recover rank-one $\bar{\Theta}_1$. Firstly, a slack variable $\xi_1 \geq 0$ is introduced to expand the size of the feasible solution $\bar{\Theta}_1$ in constraint (49). Then another relaxation variable $\mu_1 > 0$, namely penalty parameter, is introduced to the objective function. After that, problem (48) can be equivalently written as

$$\max_{t, \xi_1, \bar{\Theta}_1} t - \mu_1 \xi_1 \quad (50a)$$

$$\text{s.t. } \bar{\Theta}_1(n, n) = 1, \forall n = 1, \dots, N+1, \bar{\Theta}_1 \succeq \mathbf{0}, \quad (50b)$$

$$\text{tr}(\bar{\Theta}_1) - \lambda_{max}(\bar{\Theta}_1) \leq \xi_1, \xi_1 \geq 0, \quad (50c)$$

$$(47d), (47e), (47f). \quad (50d)$$

For any $\mu_1 > \mu_1^0$, problem (48) and (50) are equivalent, so that the two problems share the same solution. In other words, the penalty optimization solution of problem (50) is also available for problem (48). Due to the fact that convex function $\lambda_{max}(\bar{\Theta}_1)$ is not differentiable, its sub-gradient is written as $\bar{\theta}_{max}^1 (\bar{\theta}_{max}^1)^H$, where $\bar{\theta}_{max}^1$ is the eigenvector corresponding to $\lambda_{max}(\bar{\Theta}_1)$. Therefore, the first-order approximation of $\lambda_{max}(\bar{\Theta}_1)$ is taken the place of

$$\lambda_{max}(\bar{\Theta}_1) \geq \lambda_{max}(\tilde{\Theta}_1) + \text{tr}(\tilde{\theta}_{max}^1 (\tilde{\theta}_{max}^1)^H (\bar{\Theta}_1 - \tilde{\Theta}_1)), \quad (51)$$

where $\lambda_{max}(\tilde{\Theta}_1)$ is the maximum eigenvalue of the feasible solution $\tilde{\Theta}_1$, $\tilde{\theta}_{max}^1$ is the eigenvector corresponding to

$\lambda_{max}(\tilde{\Theta}_1)$. Placing the low bound of $\lambda_{max}(\bar{\Theta}_1)$ in problem (50), we have

$$\max_{t, \xi_1, \bar{\Theta}_1} t - \mu_1 \xi_1 \quad (52a)$$

$$\text{s.t. } \bar{\Theta}_1(n, n) = 1, \forall n = 1, \dots, N+1, \bar{\Theta}_1 \succeq \mathbf{0}, \quad (52b)$$

$$\text{tr}(\bar{\Theta}_1) - \lambda_{max}(\tilde{\Theta}_1) - \text{tr}(\tilde{\theta}_{max}^1 (\tilde{\theta}_{max}^1)^H (\bar{\Theta}_1 - \tilde{\Theta}_1)) \leq \xi_1, \xi_1 \geq 0, \quad (52c)$$

$$(47d), (47e), (47f). \quad (52d)$$

When μ_1 and $\tilde{\Theta}_1$ are known, the above optimization problem can be efficiently solved via CVX tool, while the rank-one solution $\bar{\Theta}_1$ is obtained.

D. Optimization of $\bar{\Theta}_2$

When \mathbf{A} and $\bar{\Theta}_1$ are fixed, the optimization problem (47) can be reduced to as follows

$$\max_{t, \bar{\Theta}_2} t \quad (53a)$$

$$\text{s.t. } \bar{\Theta}_2(n, n) = 1, \forall n = 1, \dots, N+1, \quad (53b)$$

$$\bar{\Theta}_2 \succeq \mathbf{0}, \text{rank}(\bar{\Theta}_2) = 1, \quad (53c)$$

$$2^{2t} \leq 1 + \frac{\beta_1 P \text{tr}(\bar{\Theta}_2 \mathbf{H}_2^H \mathbf{A} \mathbf{H}_1 \bar{\Theta}_1 \mathbf{H}_1^H \mathbf{A}^H \mathbf{H}_2)}{\text{tr}(\bar{\Theta}_2 \mathbf{C}_{12})}, \quad (53d)$$

$$2^{2t} \leq 1 + \frac{\beta_2 P \text{tr}(\bar{\Theta}_2 \mathbf{H}_1^H \mathbf{A} \mathbf{H}_2 \bar{\Theta}_1 \mathbf{H}_2^H \mathbf{A}^H \mathbf{H}_1)}{\text{tr}(\bar{\Theta}_2 \mathbf{C}_{21})}. \quad (53e)$$

Let us respectively define two slack variables as follow

$$\eta_{12}^i = \frac{\sqrt{\beta_1 P \text{tr}(\bar{\Theta}_2^i \mathbf{H}_2^H \mathbf{A} \mathbf{H}_1 \bar{\Theta}_1 \mathbf{H}_1^H \mathbf{A}^H \mathbf{H}_2)}}{\text{tr}(\bar{\Theta}_2^i \mathbf{C}_{12})}, \quad (54)$$

$$\eta_{21}^i = \frac{\sqrt{\beta_2 P \text{tr}(\bar{\Theta}_2^i \mathbf{H}_1^H \mathbf{A} \mathbf{H}_2 \bar{\Theta}_1 \mathbf{H}_2^H \mathbf{A}^H \mathbf{H}_1)}}{\text{tr}(\bar{\Theta}_2^i \mathbf{C}_{21})}, \quad (55)$$

where i is the iteration number. In line with GFP [34], constraint (53d) and (53e) can be changed to the following two convex constraints

$$2^{2t} \leq 1 + 2\eta_{12}^i \sqrt{\beta_1 P \text{tr}(\bar{\Theta}_2 \mathbf{H}_2^H \mathbf{A} \mathbf{H}_1 \bar{\Theta}_1 \mathbf{H}_1^H \mathbf{A}^H \mathbf{H}_2)} - (\eta_{12}^i)^2 \text{tr}(\bar{\Theta}_2 \mathbf{C}_{12}), \quad (56)$$

$$2^{2t} \leq 1 + 2\eta_{21}^i \sqrt{\beta_2 P \text{tr}(\bar{\Theta}_2 \mathbf{H}_1^H \mathbf{A} \mathbf{H}_2 \bar{\Theta}_1 \mathbf{H}_2^H \mathbf{A}^H \mathbf{H}_1)} - (\eta_{21}^i)^2 \text{tr}(\bar{\Theta}_2 \mathbf{C}_{21}). \quad (57)$$

We bring the above two inequalities in problem (53), which yields

$$\max_{t, \bar{\Theta}_2} t \quad (58a)$$

$$\text{s.t. } \bar{\Theta}_2(n, n) = 1, \forall n = 1, \dots, N+1, \quad (58b)$$

$$\bar{\Theta}_2 \succeq \mathbf{0}, \text{rank}(\bar{\Theta}_2) = 1, \quad (58c)$$

$$(56), (57). \quad (58d)$$

For the non-convex constraint $\text{rank}(\bar{\Theta}_2) = 1$, we adopt the same penalty method to process it. For brief, the related details

are omitted. By using the penalty method, problem (58) is converted to

$$\max_{t, \xi_2, \bar{\Theta}_2} t - \mu_2 \xi_2 \quad (59a)$$

$$\text{s.t. } \bar{\Theta}_2(n, n) = 1, \forall n = 1, \dots, N+1, \bar{\Theta}_2 \succeq \mathbf{0}, \quad (59b)$$

$$\begin{aligned} \text{tr}(\bar{\Theta}_2) - \lambda_{\max}(\tilde{\Theta}_2) - \text{tr}(\tilde{\theta}_{\max}^2 (\tilde{\theta}_{\max}^2)^H (\bar{\Theta}_2 - \tilde{\Theta}_2)) \\ \leq \xi_2, \xi_2 \geq 0, \end{aligned} \quad (59c)$$

$$(56), (57), \quad (59d)$$

where $\mu_2 > 0$ is a penalty parameter, $\xi_2 \geq 0$ is a slack variable, $\tilde{\theta}_{\max}^2$ is the eigenvector corresponding to the maximum eigenvalue $\lambda_{\max}(\tilde{\Theta}_2)$ of the feasible solution $\tilde{\Theta}_2$. In the same manner, problem (59) can be solved by CVX, thereby solution $\bar{\Theta}_2$ satisfying rank-one constraint can be achieved.

E. Overall algorithm

In the proposed ONS-SDP-PSCA scheme, the expression of beamforming matrix \mathbf{A} can be obtained in semi-closed form by ONS method, and IRS rank-one phase matrices $\bar{\Theta}_1$ and $\bar{\Theta}_2$ can be achieved by a SDP-PSCA-based penalty method. The detailed iterative process of the proposed ONS-SDP-PSCA scheme is presented in Algorithm 2. It is noted that the two penalty factors μ_1 and μ_2 are gradually increased in each sub-iteration of finding rank-one $\bar{\Theta}_1$ and $\bar{\Theta}_2$, when the $\zeta_{1\max}$ and $\zeta_{2\max}$ are reached, ξ_1 and ξ_2 are very small, which are considered as 0.

Algorithm 2 Proposed ONS-SDP-PSCA algorithm

- 1: Given \mathbf{A}^0 , $\bar{\Theta}_1^0$ and $\bar{\Theta}_2^0$, R^0 can be computed.
 - 2: Set the convergence error δ and initialize iteration number $i = 0$.
 - 3: **repeat**
 - 4: With $(\bar{\Theta}_1^i, \bar{\Theta}_2^i)$, calculate \mathbf{A}^{i+1} with (45) and (46).
 - 5: With $(\mathbf{A}^{i+1}, \bar{\Theta}_2^i)$, initialize μ_1^0 and $\bar{\Theta}_1^0$, set $\zeta_1 > 0$, $\zeta_{1\max}$ and $i_1 = 0$.
 - 6: **repeat**
 - 7: With $(\mu_1^{i_1}, \bar{\Theta}_1^{i_1})$, obtain $(\xi_1^{i_1+1}, \bar{\Theta}_1^{i_1+1})$ by solving problem (52).
 - 8: Update $\mu_1^{i_1+1} = \min\{\zeta_1 \mu_1^{i_1}, \zeta_{1\max}\}$ and $\bar{\Theta}_1^{i_1+1} = \bar{\Theta}_1^{i_1+1}$.
 - 9: $i_1 = i_1 + 1$.
 - 10: **until** (52) converges, and set $\bar{\Theta}_1^{i+1} = \bar{\Theta}_1^{i_1+1}$.
 - 11: With $(\mathbf{A}^{i+1}, \bar{\Theta}_1^{i+1})$, initialize μ_2^0 and $\bar{\Theta}_2^0$, set $\zeta_2 > 0$, $\zeta_{2\max}$ and $i_2 = 0$.
 - 12: **repeat**
 - 13: With $(\mu_2^{i_2}, \bar{\Theta}_2^{i_2})$, obtain $(\xi_2^{i_2+1}, \bar{\Theta}_2^{i_2+1})$ by solving problem (59).
 - 14: Update $\mu_2^{i_2+1} = \min\{\zeta_2 \mu_2^{i_2}, \zeta_{2\max}\}$ and $\bar{\Theta}_2^{i_2+1} = \bar{\Theta}_2^{i_2+1}$.
 - 15: $i_2 = i_2 + 1$.
 - 16: **until** (59) converges, and set $\bar{\Theta}_2^{i+1} = \bar{\Theta}_2^{i_2+1}$.
 - 17: Calculate R^{i+1} with $(\mathbf{A}^{i+1}, \bar{\Theta}_1^{i+1}, \bar{\Theta}_2^{i+1})$.
 - 18: $i = i + 1$.
 - 19: **until**
 - 20: $|R^{i+1} - R^i| \leq \delta$.
-

According to (45) and (46), the complexity of \mathbf{A} is denoted as $2(N+1)^3 + 4M^2N + 4MN^2 + 9M^2 - N^2 + 6MN + 14M + 3N + 3$ FLOPs. In problem (52), there exist $n_{\bar{\Theta}_1} = (N+1)^2 + 2$ variables, $N+6$ linear constraints, one linear matrix inequality (LMI) constraint of size $N+1$, its complexity is $n_{\bar{\Theta}_1} \sqrt{2N+7}[(N+1)^3 + n_{\bar{\Theta}_1}((N+1)^2 + N+6) + n_{\bar{\Theta}_1}^2 + N+6]$. Similarly, problem (59) has $N+5$ linear constraints, one linear matrix inequality (LMI) constraint of size $N+1$. The corresponding complexity is $n_{\bar{\Theta}_2} \sqrt{2N+6}[(N+1)^3 + n_{\bar{\Theta}_2}((N+1)^2 + N+5) + n_{\bar{\Theta}_2}^2 + N+5]$, where $n_{\bar{\Theta}_2} = (N+1)^2 + 2$ is the number of variables. The total complexity of ONS-SDP-PSCA algorithm is calculated as

$$\begin{aligned} \mathcal{O}\{D_2[2(N+1)^3 + 4M^2N + 4MN^2 + 9M^2 - N^2 \\ + 6MN + 14M + 3N + 3 + n_{\bar{\Theta}_1} \sqrt{2N+7}((N+1)^3 \\ + n_{\bar{\Theta}_1}((N+1)^2 + N+6) + n_{\bar{\Theta}_1}^2 + N+6) \\ + n_{\bar{\Theta}_2} \sqrt{2N+6}((N+1)^3 + n_{\bar{\Theta}_2}((N+1)^2 + N+5) \\ + n_{\bar{\Theta}_2}^2 + N+5)] \ln(1/\varepsilon)\} \end{aligned} \quad (60)$$

FLOPs, where D_2 is the iterative number in Algorithm 2.

V. NUMERICAL RESULTS ANALYSIS

To validate the convergence and rate performance of the proposed LC-ZF-SCA and ONS-SDP-PSCA schemes in this section, some numerical simulation results are presented. Assuming the coordinates of U_1 , U_2 , IRS (or UAV) and AF relay are $(0, 0, 0)$, $(0, 120\text{m}, 0)$, $(-10\text{m}, 60\text{m}, 20\text{m})$ and $(10\text{m}, 60\text{m}, 10\text{m})$ in three-dimensional (3D) space, and the path loss at distance d is computed by $PL(d) = PL_0 - 10\alpha \log_{10}(\frac{d}{d_0})$. PL_0 is the reference path loss at $d_0 = 1\text{m}$, and is generally set as -30dB . Besides, α is the path attenuation index of the channel link between transceivers. In this paper, α_{1i} , α_{1r} , α_{2i} , α_{2r} and α_{ir} respectively denote the path attenuation indexes from U_1 to IRS, from U_1 to AF relay, from U_2 to IRS, from U_2 to AF relay and from IRS to AF relay. The related parameters are chosen as follow: $\alpha_{1i} = \alpha_{2i} = \alpha_{ir} = 2.0$, $\alpha_{1r} = \alpha_{2r} = 3.6$, $\sigma_1^2 = \sigma_2^2 = \sigma_r^2 = \sigma^2 = -90\text{dBm}$, and $P_1 = P_1 = P_r = \frac{1}{3}P$, where P is the total transmit power of the IRS-assisted two-way AF relay network.

In order to better analyze the rate performance of the proposed two methods, the following two cases are regarded as the benchmark schemes.

(1) **IRS-assisted two-way AF relay with random phase:** With \mathbf{A} optimized, the phase of each IRS unit is selected randomly from the phase interval $(0, 2\pi]$.

(2) **Only AF relay:** A wireless network aided by a two-way AF relay is considered, while \mathbf{A} can be obtained by ONS method.

Fig. 2 shows the computational complexity of the proposed two methods versus the number N of IRS units with $(M, D1, D2, \varepsilon) = (2, 6, 6, 0.1)$. It is obvious that the complexity corresponding to the proposed LC-ZF-SCA and ONS-SDP-PSCA schemes gradually increase as N increase. Furthermore, since the optimization variables are matrices, the complexity of ONS-SDP-PSCA method is much higher than that of LC-ZF-SCA method with vector optimization variables.

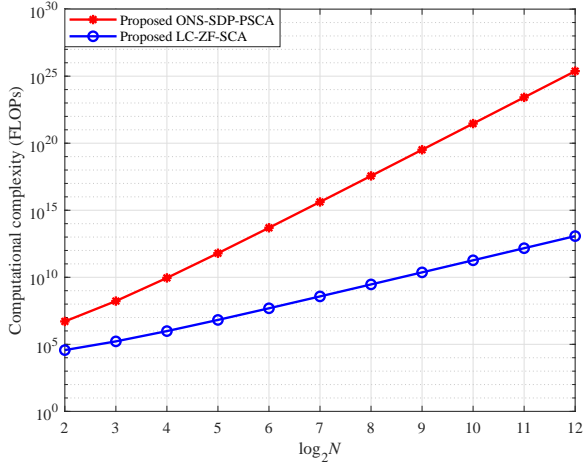


Fig. 2. Complexity versus the number of IRS units given $(M, D1, D2, \varepsilon) = (2, 6, 6, 0.1)$.

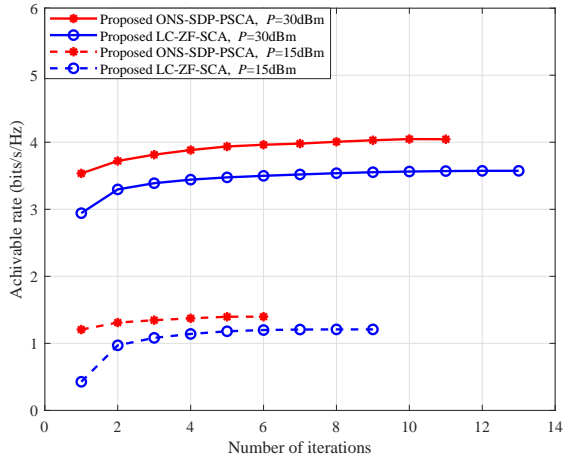


Fig. 3. Convergence of the proposed two methods given $(M, N) = (2, 128)$.

When N goes to large scale, the complexity gap between LC-ZF-SCA and ONS-SDP-PSCA widens.

Fig. 3 verifies the convergence of the proposed LC-ZF-SCA and ONS-SDP-PSCA methods at $P = 15\text{dBm}$ and $P = 30\text{dBm}$, respectively. From Fig. 3, it is clearly visible that the proposed LC-ZF-SCA and ONS-SDP-PSCA methods can gradually converge to the rate ceil within several iterations for different P . For the proposed two schemes, their convergence rates at $P = 15\text{dBm}$ are much faster than those at $P = 30\text{dBm}$. Besides, the convergence rate of ONS-SDP-PSCA scheme is faster than that of LC-ZF-SCA method for different P . Therefore, we can draw a conclusion that the proposed LC-ZF-SCA and ONS-SDP-PSCA methods are effective and feasible.

Fig. 4 presents the achievable rate versus total transmit power P given $(M, N) = (2, 128)$. As shown in Fig. 4, it is clear that the achievable rates of the proposed two schemes, called LC-ZF-SCA and ONS-SDP-PSCA, increase as total transmit power P increase. In contrast to the two benchmark schemes: random phase and only AF relay, the rate perfor-

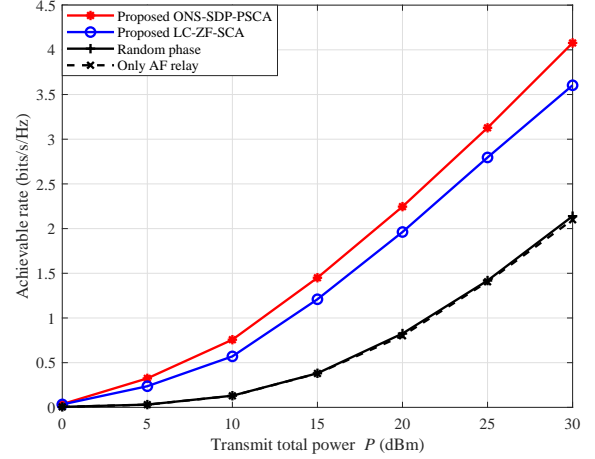


Fig. 4. Achievable rate versus total transmit power given $(M, N) = (2, 128)$.

mance enhancement obtained by LC-ZF-SCA and ONS-SDP-PSCA methods are significant in the high P region. Moreover, the proposed ONS-SDP-PSCA method perform better than the proposed LC-ZF-SCA scheme in the all P region. When $P = 30\text{dBm}$, the proposed LC-ZF-SCA and ONS-SDP-PSCA methods can respectively achieve rate performance gains of up to 90.6% and 68.5% over those of random phase and only AF relay. Furthermore, the rate performance of ONS-SDP-PSCA method is higher 0.4bits/s/Hz than that of LC-ZF-SCA method.

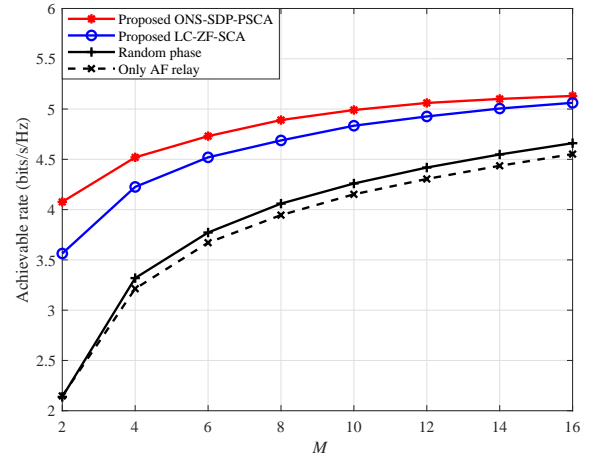


Fig. 5. Achievable rate versus the number of antennas at AF relay given $(N, P) = (128, 30\text{dBm})$.

Fig. 5 shows the achievable rate versus the number M of antennas at AF relay given $(N, P) = (128, 30\text{dBm})$. As seen in Fig. 5, the two proposed LC-ZF-SCA and ONS-SDP-PSCA methods have higher rate performance than random phase and only AF relay. As M increases, the rate performance of the two proposed methods and the two benchmark schemes increases, and the rate performance gap between the proposed two methods is slowly narrowed. Besides that, it can be

observed that the decreasing order on rate is ONS-SDP-PSCA, LC-ZF-SCA, random phase and only AF relay.

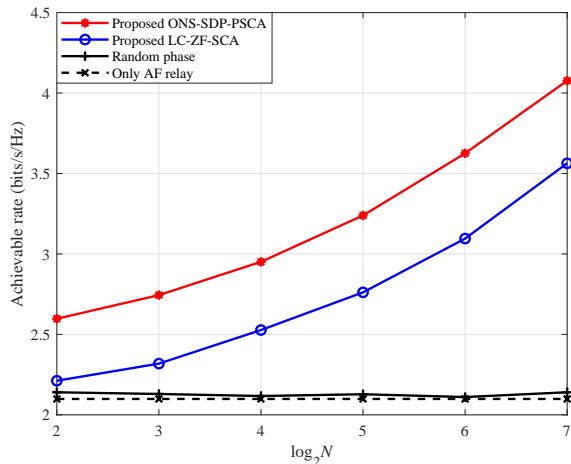


Fig. 6. Achievable rate versus the number of IRS units given $(M, P) = (2, 30\text{dBm})$.

Fig. 6 depicts the achievable rate versus the number N of IRS units for the proposed LC-ZF-SCA and ONS-SDP-PSCA methods with $(M, P) = (2, 30\text{dBm})$. Apparently, the rate performance gaps between the proposed two methods and the two benchmark schemes gradually widen as N increases, while the rates of the two benchmark schemes remain a small fluctuation. Thus, it is confirmed that optimizing AF beamforming matrix and IRS phase shifts of two time slots is necessary and effective. When N goes to medium and large scale, the rate performance gaps become especially more evident. Additionally, it can be found that the rate obtained by the proposed LC-ZF-SCA method is lower than that of the proposed ONS-SDP-PSCA method.

VI. CONCLUSIONS

An IRS-and-UAV-aided two-way AF wireless network was discussed in this paper, where two users could communicate with the help of an AF relay and an IRS attached to UAV. To solve the optimization problem of maximizing minimum rate, there existed two AI methods called LC-ZF-SCA and ONS-SDP-PSCA were proposed to jointly optimize AF beamforming matrix and IRS phase shifts for rate enhancement. As shown in simulation results, the proposed LC-ZF-SCA and ONS-SDP-PSCA methods were proved to be convergent and feasible. Compare with an IRS-assisted two-way AF relay with random phase and only an AF relay wireless networks, the achievable rate of the IRS-aided two-way AF wireless network could be significantly improved by using the proposed LC-ZF-SCA and ONS-SDP-PSCA methods. For example, at least 68.5% rate gain could be obtained by the proposed two schemes when $P=30\text{dBm}$. Furthermore, the complexity of LC-ZF-SCA method is much lower than that of ONS-SDP-PSCA method at cost of rate performance loss.

REFERENCES

- [1] X. Mu, Y. Liu, L. Guo, J. Lin, and H. V. Poor, "Intelligent reflecting surface enhanced multi-UAV NOMA networks," *IEEE J. Sel. Areas Commun.*, vol. 39, no. 10, pp. 3051–3066, Oct. 2021.
- [2] S. Jiao, F. Fang, X. Zhou, and H. Zhang, "Joint beamforming and phase shift design in downlink UAV networks with IRS-assisted NOMA," *J. Commun. Inf. Netw.*, vol. 5, no. 2, pp. 138–149, June 2020.
- [3] L. Ge, P. Dong, H. Zhang, J.-B. Wang, and X. You, "Joint beamforming and trajectory optimization for intelligent reflecting surfaces-assisted UAV communications," *IEEE Access*, vol. 8, pp. 78 702–78 712, Apr. 2020.
- [4] F. Wen, J. Shi, G. Gui, H. Gacanin, and O. A. Dobre, "3-d positioning method for anonymous UAV based on bistatic polarized MIMO radar," *IEEE Internet Things J.*, vol. 10, no. 1, pp. 815–827, Jan. 2023.
- [5] Q. Wu, J. Xu, Y. Zeng, D. W. K. Ng, N. Al-Dhahir, R. Schober, and A. L. Swindlehurst, "A comprehensive overview on 5G-and-beyond networks with UAVs: From communications to sensing and intelligence," *IEEE J. Sel. Areas Commun.*, vol. 39, no. 10, pp. 2912–2945, Oct. 2021.
- [6] L. Ruan, J. Wang, J. Chen, Y. Xu, Y. Yang, H. Jiang, Y. Zhang, and Y. Xu, "Energy-efficient multi-UAV coverage deployment in UAV networks: A game-theoretic framework," *China Commun.*, vol. 15, no. 10, pp. 194–209, Oct. 2018.
- [7] L. Diels, M. Vlaminck, B. De Wit, W. Philips, and H. Luong, "On the optimal mounting angle for a spinning LiDAR on a UAV," *IEEE Sensors J.*, vol. 22, no. 21, pp. 21 240–21 247, Nov. 2022.
- [8] T. Alladi, Naren, G. Bansal, V. Chamola, and M. Guizani, "SecAuthUAV: A novel authentication scheme for UAV-ground station and UAV-UAV communication," *IEEE Trans. Veh. Technol.*, vol. 69, no. 12, pp. 15 068–15 077, Dec. 2020.
- [9] X. Zhou, S. Yan, Q. Wu, F. Shu, and D. W. K. Ng, "Intelligent reflecting surface (IRS)-aided covert wireless communications with delay constraint," *IEEE Trans. Wireless Commun.*, vol. 21, no. 1, pp. 532–547, Jan. 2022.
- [10] Q. Wu and R. Zhang, "Intelligent reflecting surface enhanced wireless network via joint active and passive beamforming," *IEEE Trans. Wireless Commun.*, vol. 18, no. 11, pp. 5394–5409, Nov. 2019.
- [11] X. Wang, F. Shu, W. Shi, X. Liang, R. Dong, J. Li, and J. Wang, "Beamforming design for IRS-aided decode-and-forward relay wireless network," *IEEE Trans. Green Commun. Netw.*, vol. 6, no. 1, pp. 198–207, Mar. 2022.
- [12] F. Shu, L. Yang, X. Jiang, W. Cai, W. Shi, M. Huang, J. Wang, and X. You, "Beamforming and transmit power design for intelligent reconfigurable surface-aided secure spatial modulation," *IEEE J. Sel. Topics Signal Process.*, vol. 16, no. 5, pp. 933–949, Aug. 2022.
- [13] W. Shi, X. Zhou, L. Jia, Y. Wu, F. Shu, and J. Wang, "Enhanced secure wireless information and power transfer via intelligent reflecting surface," *IEEE Commun. Lett.*, vol. 25, no. 4, pp. 1084–1088, Apr. 2021.
- [14] M. Al-Jarrah, E. Alsusa, A. Al-Dweik, and D. K. C. So, "Capacity analysis of IRS-based UAV communications with imperfect phase compensation," *IEEE Wireless Commun. Lett.*, vol. 10, no. 7, pp. 1479–1483, July 2021.
- [15] A. Mahmoud, S. Muhaidat, P. C. Sofotasios, I. Abualhaol, O. A. Dobre, and H. Yanikomeroglu, "Intelligent reflecting surfaces assisted UAV communications for IoT networks: Performance analysis," *IEEE Trans. Green Commun. Netw.*, vol. 5, no. 3, pp. 1029–1040, Sep. 2021.
- [16] M. Hua, L. Yang, Q. Wu, C. Pan, C. Li, and A. L. Swindlehurst, "UAV-assisted intelligent reflecting surface symbiotic radio system," *IEEE Trans. Wireless Commun.*, vol. 20, no. 9, pp. 5769–5785, Sep. 2021.
- [17] S. Berger, M. Kuhn, A. Wittneben, T. Unger, and A. Klein, "Recent advances in amplify-and-forward two-hop relaying," *IEEE Commun. Mag.*, vol. 47, no. 7, pp. 50–56, Sep. 2009.
- [18] B. Rankov and A. Wittneben, "Achievable rate regions for the two-way relay channel," in *IEEE Int. Sym. Inf. Theory (ISIT)*, 2006, pp. 1668–1672.
- [19] E. Yilmaz, R. Zakhour, D. Gesbert, and R. Knopp, "Multi-pair two-way relay channel with multiple antenna relay station," in *IEEE Int. Conf. Commun. (ICC)*, 2010, pp. 1–5.
- [20] K. Liu, A. K. Sadek, W. Su, and A. Kwasinski, *Cooperative Communications and Networking*. Cambridge University Press, 2008.
- [21] G. Farhadi and N. Beaulieu, "On the ergodic capacity of multi-hop wireless relaying systems," *IEEE Trans. Wireless Commun.*, vol. 8, no. 5, pp. 2286–2291, May 2009.
- [22] Q. Gu, D. Wu, X. Su, J. Jin, Y. Yuan, and J. Wang, "Performance comparison between reconfigurable intelligent surface and relays: Theoretical methods and a perspective from operator," 2021. [Online]. Available: <https://arxiv.org/abs/2101.12091>

- [23] H. Feng and Y. Zhao, "Indoor enhancement of mmWave based on reconfigurable intelligent surface: IRS or DF relay connection?" in *IEEE 96th Veh. Technol. Conf. (VTC2022-Fall)*, 2022, pp. 1–6.
- [24] Y. Su, X. Pang, S. Chen, X. Jiang, N. Zhao, and F. R. Yu, "IRS-UAV relaying networks for spectrum and energy efficiency maximization," in *IEEE Int. Conf. Commun. (ICC)*, 2022, pp. 2834–2839.
- [25] Q. Sun, P. Qian, W. Duan, J. Zhang, J. Wang, and K.-K. Wong, "Ergodic rate analysis and IRS configuration for multi-IRS dual-hop DF relaying systems," *IEEE Commun. Lett.*, vol. 25, no. 10, pp. 3224–3228, Oct. 2021.
- [26] Z. T. Minson and H. M. Kwon, "Secrecy rate of relay and intelligent reflecting surface antenna-assisted MIMO," in *IEEE Military Commun. Conf. (MILCOM)*, 2022, pp. 661–666.
- [27] B. Zheng and R. Zhang, "IRS meets relaying: Joint resource allocation and passive beamforming optimization," *IEEE Wireless Commun. Lett.*, vol. 10, no. 9, pp. 2080–2084, Sep. 2021.
- [28] I. Chatzigeorgiou, "The impact of 5G channel models on the performance of intelligent reflecting surfaces and decode-and-forward relaying," in *IEEE 31st Annual Int. Symposium Pers., Indoor and Mobile Radio Commun.*, 2020, pp. 1–4.
- [29] Z. Kang, C. You, and R. Zhang, "IRS-aided wireless relaying: Deployment strategy and capacity scaling," *IEEE Wireless Commun. Lett.*, vol. 11, no. 2, pp. 215–219, Feb. 2022.
- [30] X. Wang, F. Shu, R. Chen, P. Zhang, Q. Zhang, G. Xia, W. Shi, and J. Wang, "Beamforming design for RIS-aided AF relay networks," 2023. [Online]. Available: <https://arxiv.org/abs/2302.14257>
- [31] K. Lee, V. Aravinthan, S. Moon, J. Ryou, S. Kim, C. Moon, and I. Hyun, "Low-complexity two-way AF MIMO relay strategy for wireless relay networks," in *48th Asilomar Conf. Signals, Syst. and Comput.*, 2014, pp. 235–239.
- [32] X. Guan, Q. Wu, and R. Zhang, "Joint power control and passive beamforming in IRS-assisted spectrum sharing," *IEEE Commun. Lett.*, vol. 24, no. 7, pp. 1553–1557, July 2020.
- [33] Y.-C. Liang and R. Zhang, "Optimal analogue relaying with multi-antennas for physical layer network coding," in *IEEE Int. Conf. Commun.*, 2008, pp. 3893–3897.
- [34] K. Shen and W. Yu, "Fractional programming for communication systems part II: Uplink scheduling via matching," *IEEE Trans. Signal Process.*, vol. 66, no. 10, pp. 2631–2644, May 2018.